An Adaptive Discrete Newton Method for Regularization-Free Bingham Model in Yield Stress Fluids

Arooj Fatima

arooj.fatima@math.tu-dortmund.de

Institute for Applied Mathematics and Numerics (LSIII)
TU Dortmund University

12^{th} December 2022

technische universität dortmund

fakultät für mathematik

Contents

Contents

Motivation

- Viscoplastic lubrication in transport process
- Stabilization of interfaces in multi-layer flows
- Oil/gas fracking, site-specific drug delivery, medical imaging, food, cosmetic, and pharmaceutical product manufacturing, ...

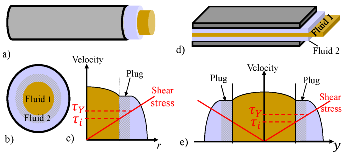

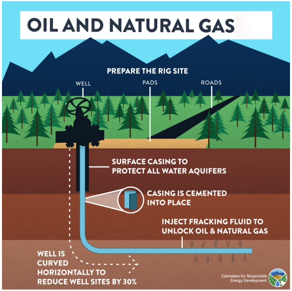

Contents

Classification of Fluids

Classification

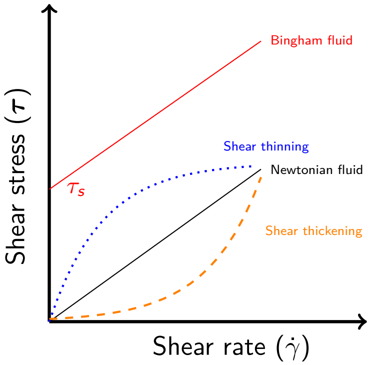

- Linear relation $\rightarrow$ Newtonian
- Otherwise $\rightarrow$ Non-Newtonian

Bingham Constitutive Law

$$\begin{cases} \boldsymbol{\tau} = 2\eta \mathbf{D}(\boldsymbol{u}) + \tau_s \dfrac{\mathbf{D}(\boldsymbol{u})}{\|\mathbf{D}(\boldsymbol{u})\|} & \text{if } \|\mathbf{D}(\boldsymbol{u})\| \neq 0 \\ \|\boldsymbol{\tau}\| \leq \tau_s & \text{if } \|\mathbf{D}(\boldsymbol{u})\| = 0 \end{cases}$$

- Applied stress $\geq$ critical value of $\tau_s \rightarrow$ Shear region
- Applied stress $\leq$ critical value of $\tau_s \rightarrow$ Rigid or plug region

Two-Field Formulation

- Viscosity model for Bingham flow

$$\eta(\|\mathbf{D}(\boldsymbol{u})\|) = 2\eta + \frac{\tau_s}{\|\mathbf{D}(\boldsymbol{u})\|}$$

- First, Shear region $\rightarrow \|\mathbf{D}(\boldsymbol{u})\| \neq 0$
- Second, Rigid or plug region $\rightarrow \|\mathbf{D}(\boldsymbol{u})\| = 0$
- Special treatment of plug zone: *Regularization*

$$\eta_\epsilon(\|\mathbf{D}(\boldsymbol{u})\|) = 2\eta + \frac{\tau_s}{\epsilon + \|\mathbf{D}(\boldsymbol{u})\|}$$ **Allouche et al.**[1]

$$\eta_\epsilon(\|\mathbf{D}(\boldsymbol{u})\|) = 2\eta + \frac{\tau_s(1 - exp(\frac{-\|\mathbf{D}(\boldsymbol{u})\|}{\epsilon}))}{\|\mathbf{D}(\boldsymbol{u})\|}$$ **Papanastasiou**[2]

Regularization Techniques

$$\eta_\epsilon(\|\mathbf{D}(\boldsymbol{u})\|) = \begin{cases} 2\eta + \dfrac{\tau_s}{\|\mathbf{D}(\boldsymbol{u})\|} & \text{if } \|\mathbf{D}(\boldsymbol{u})\| \geq \epsilon\tau_s \\ \dfrac{2\eta}{\epsilon} & \text{if } \|\mathbf{D}(\boldsymbol{u})\| \leq \epsilon\tau_s \end{cases}$$

Tanner et al.[3]

$$\boxed{\eta_\epsilon(\|\mathbf{D}(\boldsymbol{u})\|) = 2\eta + \frac{\tau_s}{\sqrt{\mathbf{D} : \mathbf{D} + \epsilon^2}}}$$

Bercovier Engelman[4]

<u>Two-Field Formulation:</u>

$$\begin{cases} -\nabla \cdot \eta_\epsilon(\|\mathbf{D}(\boldsymbol{u})\|)\mathbf{D}(\boldsymbol{u}) + \nabla p = 0 & \text{in } \Omega \\ \nabla \cdot \boldsymbol{u} = 0 & \text{in } \Omega \\ \boldsymbol{u} = \boldsymbol{g}_D & \text{on } \Gamma_D \end{cases}$$

Three-Field Formulation

Two-Field $(\boldsymbol{u}, p)$

- Solve only for non vanishing regularization parameter $\epsilon \neq 0$
- Accuracy is compromised where yield properties are important

Three-Field $(\boldsymbol{u}, \boldsymbol{\sigma}, p)$

- Introducing auxiliary stress tensor $\boldsymbol{\sigma}$
- Accurately solves regularization-free $(\epsilon = 0)$ Bingham fluid flow

Three-Field Formulation

- Bingham model with additional symmetric viscoplastic stress tensor

$$\boldsymbol{\sigma} = \frac{\mathbf{D}(\boldsymbol{u})}{\|\mathbf{D}(\boldsymbol{u})\|_{\epsilon}}$$

$$\boxed{\begin{aligned} \|\mathbf{D}(\boldsymbol{u})\|_{\epsilon}\,\boldsymbol{\sigma} - \mathbf{D}(\boldsymbol{u}) &= 0 \quad && \text{in } \Omega \\ -\nabla\cdot(2\eta\mathbf{D}(\boldsymbol{u}) + \tau_s\boldsymbol{\sigma}) + \nabla p &= 0 && \text{in } \Omega \\ \nabla\cdot\boldsymbol{u} &= 0 && \text{in } \Omega \\ \boldsymbol{u} &= \boldsymbol{g}_D && \text{on } \Gamma_D \end{aligned}}$$

- $\boldsymbol{\tau}_s$=yield stress
- $\mathbf{D}(\boldsymbol{u}) = \frac{1}{2}\left(\nabla\boldsymbol{u} + (\nabla\boldsymbol{u})^T\right)$
- η =viscosity
- $\boldsymbol{u}, p$= velocity, pressure

Weak Formulation

- Spaces for the velocity, pressure and stress
- $\mathbb{V} = \left(H_0^1(\Omega)\right)^2$, $\mathbb{Q} = L_0^2(\Omega)$, $\mathbb{M} = \left(L^2(\Omega)\right)^{2\times 2}_{\text{sym}}$

$$
\begin{aligned}
\int_\Omega \Big(\|\mathbf{D}(\boldsymbol{u})\|_\epsilon \, \boldsymbol{\sigma} : \boldsymbol{\tau} \Big)\, dx - \int_\Omega \Big(\mathbf{D}(\boldsymbol{u}) : \boldsymbol{\tau} \Big)\, dx &= 0 \quad \text{in } \Omega \\
\int_\Omega \Big(2\eta \mathbf{D}(\boldsymbol{u}) : \mathbf{D}(\boldsymbol{v}) \Big)\, dx + \int_\Omega \Big(\tau_s \mathbf{D}(\boldsymbol{v}) : \boldsymbol{\sigma} \Big)\, dx - \int_\Omega p \, \nabla \cdot \boldsymbol{v} \, dx &= 0 \quad \text{in } \Omega \\
\int_\Omega q \, \nabla \cdot \boldsymbol{u} \, dx &= 0 \quad \text{in } \Omega
\end{aligned}
$$

$$
\langle \mathcal{A}_1 \boldsymbol{u}, \boldsymbol{v} \rangle := \int_\Omega 2\eta \mathbf{D}(\boldsymbol{u}) : \mathbf{D}(\boldsymbol{v})\, dx \quad , \quad \langle \mathcal{A}_2 \boldsymbol{\sigma}, \boldsymbol{\tau} \rangle = \int_\Omega \tau_s \|\mathbf{D}(\boldsymbol{u})\|_\epsilon \boldsymbol{\sigma} : \boldsymbol{\tau}\, dx
$$

$$
\langle \mathcal{B}_1 \boldsymbol{v}, q \rangle := -\int_\Omega \nabla \cdot \boldsymbol{v} \;\, q \, dx \quad , \quad \langle \mathcal{B}_2 \boldsymbol{v}, \boldsymbol{\sigma} \rangle := -\int_\Omega \tau_s \mathbf{D}(\boldsymbol{v}) : \boldsymbol{\sigma}\, dx
$$

Weak Formulation

$$\langle \mathcal{A}(\boldsymbol{u},\boldsymbol{\sigma}),(\boldsymbol{v},\boldsymbol{\tau})\rangle = \langle \mathcal{A}_1\boldsymbol{u},\boldsymbol{v}\rangle + \langle \mathcal{A}_2\boldsymbol{\sigma},\boldsymbol{\tau}\rangle + \left\langle \mathcal{B}_2^{\mathsf{T}}\boldsymbol{v},\boldsymbol{\sigma}\right\rangle + \langle \mathcal{B}_2\boldsymbol{u},\boldsymbol{\tau}\rangle$$

$$\begin{bmatrix} \mathcal{A}_1 & \mathcal{B}_2^{\mathsf{T}} & \mathcal{B}_1^{\mathsf{T}} \\ \mathcal{B}_2 & -\mathcal{A}_2 & \mathbf{0} \\ \mathcal{B}_1 & \mathbf{0} & \mathbf{0} \end{bmatrix} \begin{bmatrix} \boldsymbol{u} \\ \boldsymbol{\sigma} \\ p \end{bmatrix} = \begin{bmatrix} rhs_{\boldsymbol{u}} \\ rhs_{\boldsymbol{\sigma}} \\ rhs_p \end{bmatrix}$$

The associated bilinear form for $\mathcal{U} = (\boldsymbol{u},\boldsymbol{\sigma})$ and $\mathcal{V} = (\boldsymbol{v},\boldsymbol{\tau})$ as

$$a(\mathcal{U},\mathcal{V}) = a_1(\boldsymbol{u},\boldsymbol{v}) + a_2(\boldsymbol{\sigma},\boldsymbol{\tau}) + b_2(\boldsymbol{v},\boldsymbol{\sigma}) + b_2(\boldsymbol{u},\boldsymbol{\tau})$$

Find $(\mathcal{U},p) \in \mathbb{X}\times\mathbb{Q}$ such that:

$$\begin{cases} a(\mathcal{U},\mathcal{V}) + b(\mathcal{V},p) = \langle \boldsymbol{f},\mathcal{V}\rangle & \forall \mathcal{V}\in\mathbb{X} \\ b(\mathcal{U},q) \qquad\qquad\quad = \langle \boldsymbol{g},q\rangle & \forall q\in\mathbb{Q} \end{cases} \tag{1}$$

Contents

Finite Element Discretization

- Domain $\Omega \subset \mathbb{R}^d \longrightarrow$ grid $\mathcal{T}^h$ consisting of elements $K \in \mathcal{T}^h$
- Approximation spaces

$$\mathbb{V}^h = \left\{ \boldsymbol{v}_h \in \mathbb{V}, \boldsymbol{v}_{h|K} \in (Q_2(K))^2 \right\}$$
$$\mathbb{M}^h = \left\{ \boldsymbol{\tau}_h \in \mathbb{M}, \boldsymbol{\sigma}_{h|K} \in (Q_2(K))^{2\times 2} \right\}$$
$$\mathbb{Q}^h = \left\{ q_h \in \mathbb{Q}, q_{h|K} \in P_1^{\text{disc}}(K) \right\}$$

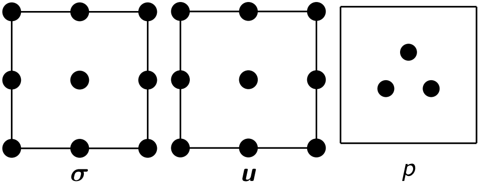

Contents

Newton Method

Algorithm

- Provide the input parameters, e.g. tolerance, parameters of the non-linear solver, initial guess and the iteration number n
- Repeat until the tolerance is achieved
- Calculate the residual $\mathcal{R}(\mathcal{U}^n) = A\,\mathcal{U}^n - b$
- Build the Jacobian $J(\mathcal{U}^n) = \frac{\partial \mathcal{R}(\mathcal{U}^n)}{\partial \mathcal{U}^n}$
- Solve $J(\mathcal{U}^n)\;\delta\mathcal{U}^n = \mathcal{R}(\mathcal{U}^n)$
- Find the optimal value of the damping factor $\omega^n \in (-1, 0]$
- Approximate $\mathcal{U}^{n+1} = \mathcal{U}^n - \omega^n\;\delta\mathcal{U}^n$

Sensitive parameters: initial guess, damping factor ω

Discrete Newton Method

$$J(\mathcal{U}^n)=\begin{bmatrix} \dfrac{\partial R_{\boldsymbol{u}}(\mathcal{U}^n)}{\partial \boldsymbol{u}} & \dfrac{\partial R_{\boldsymbol{u}}(\mathcal{U}^n)}{\partial \boldsymbol{\sigma}} & \dfrac{\partial R_{\boldsymbol{u}}(\mathcal{U}^n)}{\partial p} \\ \dfrac{\partial R_{\boldsymbol{\sigma}}(\mathcal{U}^n)}{\partial \boldsymbol{u}} & \dfrac{\partial R_{\boldsymbol{\sigma}}(\mathcal{U}^n)}{\partial \boldsymbol{\sigma}} & \dfrac{\partial R_{\boldsymbol{\sigma}}(\mathcal{U}^n)}{\partial p} \\ \dfrac{\partial R_p(\mathcal{U}^n)}{\partial \boldsymbol{u}} & \dfrac{\partial R_p(\mathcal{U}^n)}{\partial \boldsymbol{\sigma}} & \dfrac{\partial R_p(\mathcal{U}^n)}{\partial p} \end{bmatrix}$$

Jacobian calculation method

Analytical $\longrightarrow$ Knowledge of the Jacobian a priori

Approximation $\longrightarrow$ Black box manner

$$\left[\frac{\partial \mathcal{R}(\mathcal{U}^n)}{\partial \mathcal{U}^n}\right]_j \approx \frac{\mathcal{R}(\mathcal{U}^n + \chi\delta_j) - \mathcal{R}(\mathcal{U}^n - \chi\delta_j)}{2\chi}$$

Contents

Bingham Flow in a Channel

- **Channel domain:** Unit square $\Omega = [0,1]^2$
- **Boundary conditions:** Dirichlet[5]
- $u_y = 0,\ p = -x + c,\ \eta = 1$

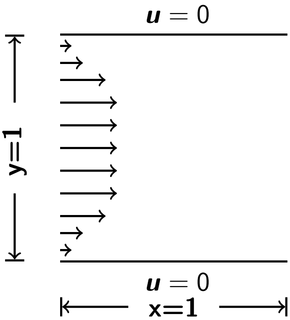

$$u_x = \begin{cases} \frac{1}{8}\left[(h-2\tau_s)^2 - (h-2\tau_s-2y)^2\right], & 0 \le y < \frac{h}{2} - \tau_s, \\ \frac{1}{8}(h-2\tau_s)^2, & \frac{h}{2} - \tau_s \le y \le \frac{h}{2} + \tau_s, \\ \frac{1}{8}\left[(h-2\tau_s)^2 - (2y-2\tau_s-h)^2\right], & \frac{h}{2} + \tau_s < y \le h. \end{cases}$$

Bingham Flow in a Channel

Two-field (u, p) formulation $\epsilon = 0$ not solve-able

ϵ	Level	NL	$\|u - u_{ex}\|$	ϵ	NL	$\|u - u_{ex}\|$
10^{-1}	3	3	3.346×10^{-3}	10^{-2}	9	1.760×10^{-3}
	4	3	2.790×10^{-3}		6	1.041×10^{-3}
	5	2	2.563×10^{-3}		3	6.771×10^{-4}

Three-field (u, σ, p) formulation $\epsilon = 0$ solved

ϵ	Level	NL	$\|u - u_{ex}\|$
10^{-1}	3	6	2.598×10^{-3}
	4	3	2.597×10^{-3}
	5	2	2.597×10^{-3}
10^{-2}	3	45	5.873×10^{-4}
	4	4	5.818×10^{-4}
	5	3	5.815×10^{-4}
10^{-3}	3	14	6.257×10^{-5}
	4	6	6.415×10^{-5}
	5	4	6.416×10^{-5}

ϵ	Level	NL	$\|u - u_{ex}\|$
10^{-4}	3	49	6.407×10^{-6}
	4	5	6.262×10^{-6}
	5	4	6.298×10^{-6}
10^{-5}	3	39	6.788×10^{-7}
	4	13	6.378×10^{-7}
	5	5	6.297×10^{-7}
0	3	18	2.000×10^{-11}
	4	4	7.000×10^{-12}
	5	3	4.000×10^{-12}

Bingham Flow in a Channel

- Velocity for $\tau_s = 0.25$

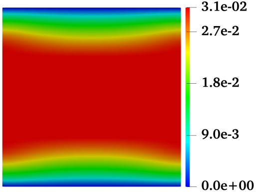

(a) $\epsilon = 10^{-1}$

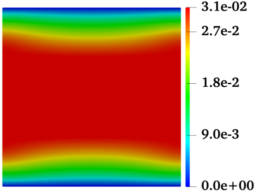

(b) $\epsilon = 10^{-2}$

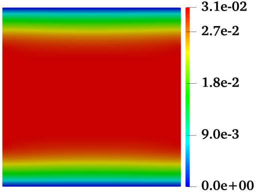

(c) $\epsilon = 10^{-3}$

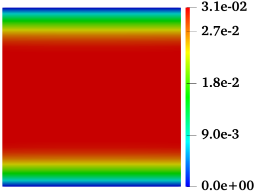

(d) $\epsilon = 10^{-4}$

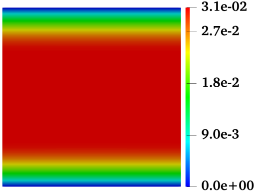

(e) $\epsilon = 10^{-5}$

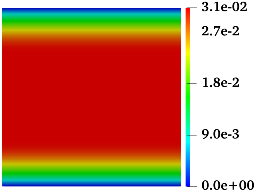

(f) $\epsilon = 0$

Bingham Flow in a Channel

- Pressure distribution and contours for $\tau_s = 0.25$

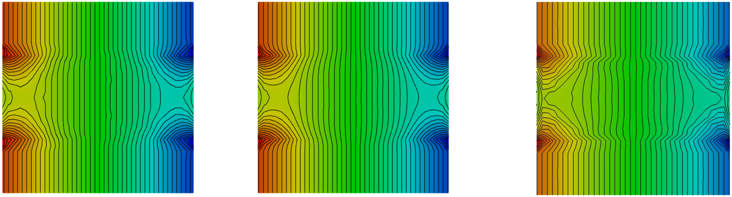

(a) $\epsilon = 10^{-4}$ (b) $\epsilon = 10^{-5}$ (c) $\epsilon = 0$

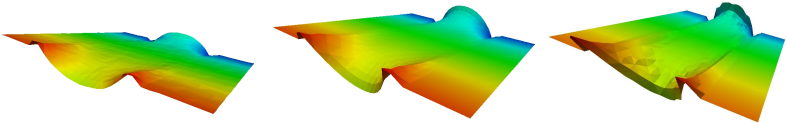

(d) $\epsilon = 10^{-4}$ (e) $\epsilon = 10^{-5}$ (f) $\epsilon = 0$

Bingham Flow in a Channel

- $\|\mathbf{D}\|$ for $\tau_s = 0.25$

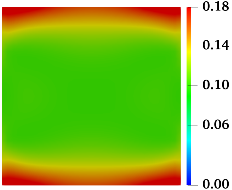

(a) $\epsilon = 10^{-1}$

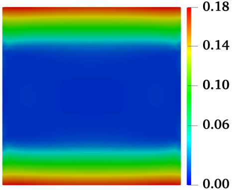

(b) $\epsilon = 10^{-2}$

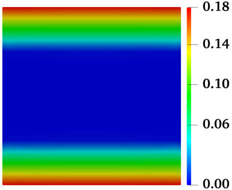

(c) $\epsilon = 10^{-3}$

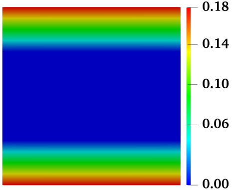

(d) $\epsilon = 10^{-4}$

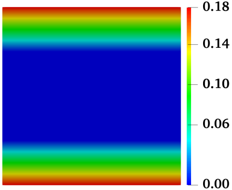

(e) $\epsilon = 10^{-5}$

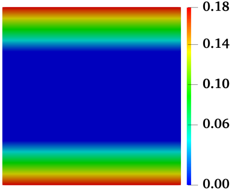

(f) $\epsilon = 0$

Bingham Flow in a Channel

Boundary conditions: Pressure drop[6,7]

$$
\begin{aligned}
u_2 &= 0 && \text{at inflow and outflow} \\
\boldsymbol{u} &= 0 && \text{at upper and lower walls} \\
\boldsymbol{\tau n.n} &= LC && \text{at inflow} \\
\boldsymbol{\tau n.n} &= 0 && \text{at outflow}
\end{aligned}
$$

- L=1
- $C = \frac{\partial p}{\partial x}$
- $\boldsymbol{n}$=unit normal vector

Exact solution for velocity[8,5] :

$$
u_1 = \begin{cases} \frac{C}{2\eta} y(1-y) - \frac{\tau_s}{\eta} y & 0 \leq y < \frac{1}{2} - \frac{\tau_s}{C} \\ \frac{C}{2\eta} (\frac{1}{2} - \frac{\tau_s}{\eta})^2 & \frac{1}{2} - \frac{\tau_s}{C} \leq y \leq \frac{1}{2} + \frac{\tau_s}{C} \\ \frac{C}{2\eta} y(1-y) - \frac{\tau_s}{\eta}(1-y) & \frac{1}{2} + \frac{\tau_s}{C} < y \leq 1 \end{cases} \tag{2}
$$

Exact solution for pressure[8,5] :

$$
p(x, y) = -C(x - L) \tag{3}
$$

Bingham Flow in a Channel

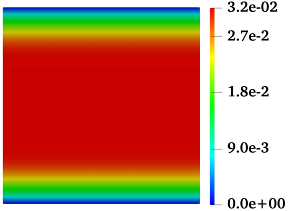

(a) $\|\boldsymbol{u}\|, \epsilon = 10^{-3}$

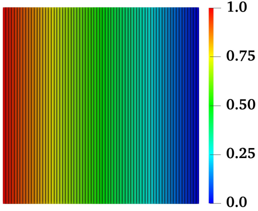

(b) $p, \epsilon = 10^{-3}$

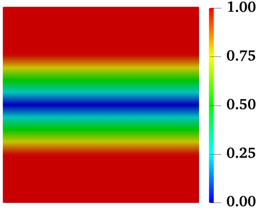

(c) $\|\boldsymbol{\sigma}\|, \epsilon = 10^{-3}$

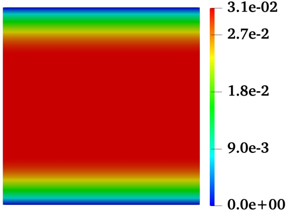

(d) $\|\boldsymbol{u}\|, \epsilon = 0$

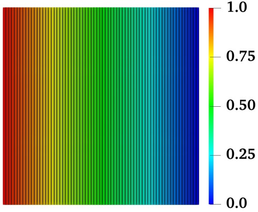

(e) $p, \epsilon = 0$

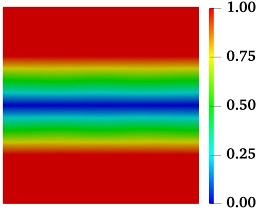

(f) $\|\boldsymbol{\sigma}\|, \epsilon = 0$

Bingham Flow in a Channel

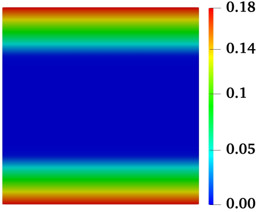

(a) $\|\mathbf{D}\|, \epsilon = 10^{-3}$

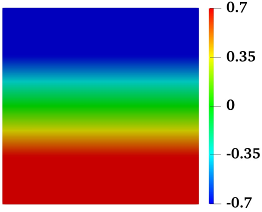

(b) $\sigma_{12}, \epsilon = 10^{-3}$

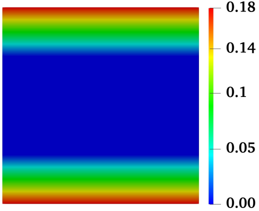

(c) $\|\mathbf{D}\|, \epsilon = 0$

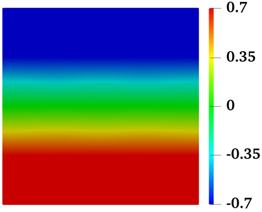

(d) $\sigma_{12}, \epsilon = 0$

exact solution is obtained!

Bingham Flow in a Channel

Three-field $(\boldsymbol{u}, \boldsymbol{\sigma}, p)$ formulation $\epsilon = 0$

DOF	L	NL	$\|\boldsymbol{u} - \boldsymbol{u}_{ex}\|_{L^2}$	$\|\boldsymbol{u} - \boldsymbol{u}_{ex}\|_{H^1}$
4741	3	6	$3.43509e-08$	$2.49700e-06$
18309	4	6	$1.63979e-08$	$1.32702e-06$
71941	5	5	$1.63729e-08$	$8.92504e-07$

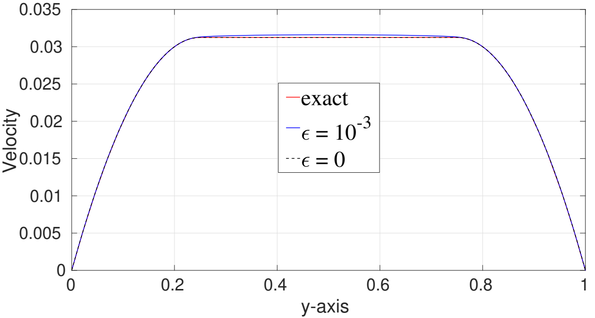

Bingham Flow in a Channel

- Newton-Multigrid solver behaviour for $\tau_s = 0.25$

ϵ	Level	NL/L	$\|u - u_{ex}\|$
10^{-1}	3	6/1	2.598×10^{-3}
	4	3/1	2.597×10^{-3}
	5	2/1	2.597×10^{-3}
	6	2/1	2.597×10^{-3}
10^{-2}	3	5/1	5.873×10^{-4}
	4	4/1	5.818×10^{-4}
	5	3/1	5.815×10^{-4}
	6	3/1	5.815×10^{-4}
10^{-3}	3	8/7	6.257×10^{-5}
	4	4/7	6.415×10^{-5}
	5	6/9	6.416×10^{-5}
	6	4/9	6.394×10^{-5}

Problem in convergence for small value of regularization parameter ϵ.

Possible Remedy: Add EOFEM or artificial diffusion stabilization

$j_{\boldsymbol{u}}(\boldsymbol{u}_h, \boldsymbol{v}_h) = \sum_{E \in \mathcal{E}_h^i} \gamma_u h \int_E [\nabla \boldsymbol{u}_h] : [\nabla \boldsymbol{v}_h] \, d\Omega$

$j_{\boldsymbol{\sigma}}(\boldsymbol{\sigma}_h, \boldsymbol{\tau}_h) = \sum_{E \in \mathcal{E}_h^i} \gamma_{\boldsymbol{\sigma}} h \int_E [\nabla \boldsymbol{\sigma}_h] : [\nabla \boldsymbol{\tau}_h] \, d\Omega$

Bingham Flow in a Channel

- Newton solver $\rightarrow$ EOFEM($\boldsymbol{u}$) $\gamma_u h$, $\gamma_u = 10^{-1}$ for $\tau_s = 0.25$

ϵ	Level	NL	$\|u - u_{ex}\|$	NL	$\|u - u_{ex}\|$
			No stab.		**stab.**
10^{-1}	2	6	2.641×10^{-3}	6	2.627×10^{-3}
	3	3	2.598×10^{-3}	3	2.598×10^{-3}
	4	2	2.596×10^{-3}	3	2.597×10^{-3}
	5	2	2.597×10^{-3}	2	2.597×10^{-3}
10^{-2}	2	9	6.079×10^{-4}	9	6.130×10^{-4}
	3	5	5.873×10^{-4}	5	5.893×10^{-4}
	4	4	5.818×10^{-4}	4	5.819×10^{-4}
	5	4	5.815×10^{-4}	3	5.815×10^{-4}

ϵ	Level	NL	$\|u - u_{ex}\|$	NL	$\|u - u_{ex}\|$
			No stab.		**stab.**
10^{-3}	2	19	6.237×10^{-5}	15	6.228×10^{-5}
	3	7	6.257×10^{-5}	5	6.296×10^{-5}
	4	5	6.415×10^{-5}	5	6.426×10^{-5}
	5	4	6.416×10^{-5}	5	6.418×10^{-5}
10^{-4}	2	15	7.835×10^{-6}	14	7.564×10^{-6}
	3	14	6.407×10^{-6}	9	6.300×10^{-6}
	4	4	6.262×10^{-6}	5	6.265×10^{-6}
	5	4	6.298×10^{-6}	4	6.308×10^{-6}

EOFEM stabilization does not effect the solution accuracy!

Bingham Flow in a Channel

- Newton-Multigrid solver $\rightarrow$ EOFEM($\boldsymbol{u}$) $\gamma_u h$, $\gamma_u = 10^{-1}$ for $\tau_s = 0.25$

ϵ	Level	NL	$\|u - u_{ex}\|$	NL	$\|u - u_{ex}\|$
		No stab.		**stab.**	
10^{-1}	2	6/1	2.641×10^{-3}	6/1	2.627×10^{-3}
	3	4/1	2.598×10^{-3}	4/1	2.598×10^{-3}
	4	3/1	2.596×10^{-3}	3/1	2.597×10^{-3}
	5	3/1	2.597×10^{-3}	3/1	2.597×10^{-3}
10^{-2}	2	9/1	6.079×10^{-4}	9/1	6.130×10^{-4}
	3	5/1	5.873×10^{-4}	5/1	5.893×10^{-4}
	4	4/1	5.818×10^{-4}	4/2	5.819×10^{-4}
	5	4/1	5.815×10^{-4}	3/1	5.814×10^{-4}

ϵ	Level	NL	$\|u - u_{ex}\|$	NL	$\|u - u_{ex}\|$
		No stab.		**stab.**	
10^{-3}	2	15/1	6.237×10^{-5}	15/1	6.228×10^{-5}
	3	7/7	6.257×10^{-5}	6/2	6.296×10^{-5}
	4	4/3	6.415×10^{-5}	5/1	6.426×10^{-5}
	5	4/4	6.416×10^{-5}	5/2	6.418×10^{-5}
10^{-4}	2			14/1	6.228×10^{-6}
	3			12/4	6.504×10^{-6}
	4			10/7	6.339×10^{-6}
	5			11/8	6.338×10^{-6}

EOFEM stabilization helped MG to solve smaller ϵ!

Bingham Flow in a Channel

- Newton-Multigrid solver $\rightarrow$ EOFEM($\boldsymbol{u}$) $\gamma_u h^2$, $\gamma_u = 10^{-1}$ for $\tau_s = 0.25$

		Newton		Newton-MG	
ϵ	Level	NL	$\|u - u_{ex}\|$	NL/L	$\|u - u_{ex}\|$
10^{-1}	2	5	2.621×10^{-3}	5/1	2.621×10^{-3}
	3	2	2.597×10^{-3}	4/1	2.598×10^{-3}
	4	2	2.596×10^{-3}	3/1	2.597×10^{-3}
	5	1	2.597×10^{-3}	2/1	2.597×10^{-3}
10^{-2}	2	7	6.100×10^{-4}	7/1	6.100×10^{-4}
	3	2	5.779×10^{-4}	5/1	5.876×10^{-4}
	4	2	5.794×10^{-4}	4/1	5.818×10^{-4}
	5	2	5.808×10^{-4}	3/1	5.815×10^{-4}

		Newton		Newton-MG	
ϵ	Level	NL	$\|u - u_{ex}\|$	NL/L	$\|u - u_{ex}\|$
10^{-3}	2	11	6.234×10^{-5}	11/1	6.234×10^{-5}
	3	3	6.258×10^{-5}	6/2	6.262×10^{-5}
	4	4	6.415×10^{-5}	5/2	6.415×10^{-5}
	5	3	6.415×10^{-5}	5/3	6.416×10^{-5}
10^{-4}	2	13	7.713×10^{-6}	13/1	7.713×10^{-6}
	3	2	5.481×10^{-6}	8/7	6.382×10^{-6}
	4	2	6.139×10^{-6}	7/9	6.265×10^{-6}
	5	1	6.297×10^{-6}	8/18	6.298×10^{-6}

Adding $\gamma_u\ h^2$ $\rightarrow$ non-linear iterations slightly reduced

Bingham Flow in a Channel

- Newton-Multigrid solver $\rightarrow$ EOFEM($\boldsymbol{\sigma}$) $\gamma_{\boldsymbol{\sigma}} h$, $\gamma_{\boldsymbol{\sigma}} = 10^{-2}$ for $\tau_s = 0.25$

ϵ	Level	NL/L	$\|u - u_{ex}\|$	NL/L	$\|u - u_{ex}\|$
		No stab.		**stab.**	
10^{-1}	2	6/1	2.641×10^{-3}	3/1	2.616×10^{-3}
	3	4/1	2.598×10^{-3}	4/1	2.598×10^{-3}
	4	3/1	2.596×10^{-3}	3/1	2.597×10^{-3}
	5	3/1	2.597×10^{-3}	3/1	2.597×10^{-3}
10^{-2}	2	9/1	6.079×10^{-4}	3/1	6.018×10^{-4}
	3	5/1	5.873×10^{-4}	4/1	5.874×10^{-4}
	4	4/1	5.818×10^{-4}	5/1	5.819×10^{-4}
	5	4/1	5.815×10^{-4}	4/2	5.815×10^{-4}

ϵ	Level	NL/L	$\|u - u_{ex}\|$	NL/L	$\|u - u_{ex}\|$
		No stab.		**stab.**	
10^{-3}	2	15/1	6.237×10^{-5}	15/1	6.257×10^{-5}
	3	7/7	6.257×10^{-5}	6/3	6.287×10^{-5}
	4	4/3	6.415×10^{-5}	6/2	6.437×10^{-5}
	5	4/4	6.416×10^{-5}	5/4	6.417×10^{-5}
10^{-4}	2			21/1	8.919×10^{-6}
	3			7/7	6.650×10^{-6}
	4			7/4	6.985×10^{-6}
	5			6/6	6.900×10^{-6}
10^{-5}	2			9/1	9.772×10^{-7}
	3			5/1	2.743×10^{-6}
	4			11/34	3.003×10^{-6}

EOFEM stabilization helped MG to solve more smaller ϵ!

Bingham Flow in a Channel

- Artificial diff. stab. $\gamma_{\boldsymbol{\sigma}} h^2 \nabla^2 \boldsymbol{\sigma}$, $\gamma_{\boldsymbol{\sigma}} = 10^{-2}$ for $\tau_s = 0.25$

Level	NL	$\|u - u_{ex}\|$	NL/L	$\|u - u_{ex}\|$
$\epsilon = 10^{-1}$				
2	5	2.633×10^{-3}	5/1	2.633×10^{-3}
3	3	2.621×10^{-3}	3/2	2.621×10^{-3}
4	3	2.607×10^{-3}	3/4	2.607×10^{-3}
5	2	2.601×10^{-3}	2/5	2.601×10^{-3}
6	2	2.598×10^{-3}	2/5	2.598×10^{-3}
$\epsilon = 10^{-2}$				
2	7	1.384×10^{-3}	7/1	1.384×10^{-3}
3	4	8.964×10^{-4}	4/6	8.964×10^{-4}
4	3	6.887×10^{-4}	3/3	6.887×10^{-4}
5	2	6.159×10^{-4}	3/4	6.159×10^{-4}
6	2	5.919×10^{-4}	3/5	5.919×10^{-4}
$\epsilon = 10^{-3}$				
2	7	1.245×10^{-3}	7/1	1.245×10^{-3}
3	4	5.811×10^{-4}	5/9	5.811×10^{-4}
4	4	2.326×10^{-4}	4/8	2.326×10^{-4}
5	4	1.107×10^{-4}	3/6	1.107×10^{-4}
6	4	7.725×10^{-5}	3/8	7.725×10^{-5}

Level	NL	$\|u - u_{ex}\|$	NL/L	$\|u - u_{ex}\|$
$\epsilon = 10^{-4}$				
2	7	1.243×10^{-3}	7/1	1.243×10^{-3}
3	4	5.724×10^{-4}	4/6	5.724×10^{-4}
4	4	2.056×10^{-4}	4/5	2.056×10^{-4}
5	4	6.740×10^{-5}	4/6	6.740×10^{-5}
6	4	2.670×10^{-5}	5/6	2.670×10^{-5}
$\epsilon = 10^{-5}$				
2	7	1.243×10^{-3}	7/1	1.243×10^{-3}
3	4	5.724×10^{-4}	6/2	5.724×10^{-4}
4	4	2.056×10^{-4}	4/3	2.056×10^{-4}
5	4	6.636×10^{-5}	4/5	6.636×10^{-5}
6	4	2.458×10^{-5}	5/6	2.458×10^{-5}
$\epsilon = 0$				
2	3	1.243×10^{-3}	3/1	1.243×10^{-3}
3	3	5.724×10^{-4}	4/1	5.724×10^{-4}
4	3	2.056×10^{-4}	5/2	2.056×10^{-4}
5	3	6.635×10^{-5}	5/2	6.635×10^{-5}
6	6	2.459×10^{-5}	6/9	2.459×10^{-5}

Regularization-free Bingham

Bingham Flow in a Channel

- Artificial diff. stab. $\gamma_{\boldsymbol{\sigma}} h^2 \nabla^2 \boldsymbol{\sigma}$, $\gamma_{\boldsymbol{\sigma}} = 10^{-3}$ for $\tau_s = 0.25$

Level	NL	$\|u - u_{ex}\|$	NL/L	$\|u - u_{ex}\|$
$\epsilon = 10^{-1}$				
2	6	2.648×10^{-3}	6/1	2.648×10^{-3}
3	3	2.603×10^{-3}	3/2	2.603×10^{-3}
4	2	2.598×10^{-3}	3/2	2.598×10^{-3}
5	2	2.597×10^{-3}	2/4	2.597×10^{-3}
6	2	2.597×10^{-3}	2/4	2.597×10^{-3}
$\epsilon = 10^{-2}$				
2	8	7.764×10^{-4}	8/1	7.764×10^{-4}
3	3	6.364×10^{-4}	3/2	6.364×10^{-4}
4	3	5.974×10^{-4}	3/3	5.974×10^{-4}
5	3	5.860×10^{-4}	3/3	5.860×10^{-4}
6	2	5.827×10^{-4}	2/4	5.827×10^{-4}
$\epsilon = 10^{-3}$				
2	9	3.457×10^{-4}	9/1	3.457×10^{-4}
3	4	1.452×10^{-4}	4/2	1.452×10^{-4}
4	4	8.630×10^{-5}	4/2	8.630×10^{-5}
5	4	7.022×10^{-5}	4/3	7.022×10^{-5}
6	5	6.569×10^{-5}	4/4	6.569×10^{-5}

Level	NL	$\|u - u_{ex}\|$	NL/L	$\|u - u_{ex}\|$
$\epsilon = 10^{-4}$				
2	9	3.306×10^{-4}	10/1	3.306×10^{-4}
3	6	1.117×10^{-4}	6/4	1.117×10^{-4}
4	7	4.155×10^{-5}	5/5	4.155×10^{-5}
5	5	1.787×10^{-5}	7/6	1.787×10^{-5}
6	6	9.418×10^{-6}	6/8	9.418×10^{-6}
$\epsilon = 10^{-5}$				
2	17	3.304×10^{-4}	17/1	3.304×10^{-4}
3	7	1.112×10^{-4}	6/4	1.112×10^{-4}
4	6	4.041×10^{-5}	5/3	4.041×10^{-5}
5	5	1.563×10^{-5}	7/6	1.563×10^{-5}
6	6	5.840×10^{-6}	7/8	5.840×10^{-6}
$\epsilon = 0$				
2	3	3.304×10^{-4}	3/1	3.304×10^{-4}
3	4	1.112×10^{-4}	6/2	1.112×10^{-4}
4	4	4.040×10^{-5}	6/4	4.040×10^{-5}
5	5	1.557×10^{-5}	6/11	1.557×10^{-5}
6	11	5.694×10^{-6}	12/22	5.694×10^{-6}

$\gamma = 10^{-3} \longrightarrow$ Regularization-free Bingham

Bingham Flow in a Channel

- Artificial diff. stab. $\gamma_{\boldsymbol{\sigma}} h^2 \nabla^2 \boldsymbol{\sigma}$, $\gamma_{\boldsymbol{\sigma}} = 10^{-4}$ for $\tau_s = 0.25$

Level	NL	$\|u - u_{ex}\|$	NL/L	$\|u - u_{ex}\|$
$\epsilon = 10^{-1}$				
2	6	2.642×10^{-3}	6/1	2.642×10^{-3}
3	3	2.599×10^{-3}	3/2	2.599×10^{-3}
4	3	2.597×10^{-3}	3/3	2.597×10^{-3}
5	2	2.597×10^{-3}	2/3	2.597×10^{-3}
6	2	2.597×10^{-3}	2/3	2.597×10^{-3}
$\epsilon = 10^{-2}$				
2	9	6.232×10^{-4}	9/1	6.232×10^{-4}
3	5	5.937×10^{-4}	5/4	5.937×10^{-4}
4	4	5.836×10^{-4}	4/3	5.836×10^{-4}
5	4	5.820×10^{-4}	4/4	5.820×10^{-4}
6	3	5.816×10^{-4}	3/4	5.816×10^{-4}
$\epsilon = 10^{-3}$				
2	21	9.234×10^{-5}	21/1	9.234×10^{-5}
3	6	7.413×10^{-5}	7/6	7.413×10^{-5}
4	5	6.728×10^{-5}	8/9	6.728×10^{-5}
5	5	6.486×10^{-5}	6/8	6.486×10^{-5}
6	6	6.414×10^{-5}	6/12	6.414×10^{-5}

Level	NL	$\|u - u_{ex}\|$	NL/L	$\|u - u_{ex}\|$
$\epsilon = 10^{-4}$				
2	29	4.428×10^{-5}	24/1	4.428×10^{-5}
3	6	2.418×10^{-5}	12/11	2.418×10^{-5}
4	6	1.299×10^{-5}	11/4	1.299×10^{-5}
5	8	8.243×10^{-6}	10/4	8.243×10^{-6}
6	5	7.023×10^{-6}	9/4	7.023×10^{-6}
$\epsilon = 10^{-5}$				
2	12	4.304×10^{-5}	12/1	4.304×10^{-5}
3	3	2.226×10^{-5}	4/11	2.224×10^{-5}
4	5	1.075×10^{-5}	6/12	1.062×10^{-5}
5	9	4.953×10^{-6}	13/28	4.567×10^{-6}
6	10	2.577×10^{-6}	16/47	2.313×10^{-6}
$\epsilon = 0$				
2	4	4.292×10^{-5}	4/1	4.292×10^{-5}
3	5	2.225×10^{-5}	6/7	2.225×10^{-5}
4	6	1.012×10^{-5}	7/6	1.012×10^{-5}
5	10	4.448×10^{-6}	13/15	4.448×10^{-6}

$\gamma = 10^{-4} \longrightarrow$ Regularization-free Bingham

Bingham Flow in a Channel

- Artificial diff. stab. $\gamma_{\boldsymbol{\sigma}} h^3 \nabla^2 \boldsymbol{\sigma}$, $\gamma_{\boldsymbol{\sigma}} = 10^{-3}$

ϵ	Level	NL	$\lVert u - u_{ex} \rVert$	NL/L	$\lVert u - u_{ex} \rVert$
10^{-1}	2	3	2.651×10^{-3}	3/1	2.651×10^{-3}
	3	2	2.604×10^{-3}	3/1	2.604×10^{-3}
	4	2	2.598×10^{-3}	3/1	2.598×10^{-3}
	5	1	2.597×10^{-3}	2/1	2.597×10^{-3}
	6	1	2.597×10^{-3}	3/2	2.597×10^{-3}
10^{-2}	2	6	9.336×10^{-4}	6/1	9.336×10^{-4}
	3	2	6.465×10^{-4}	5/1	6.465×10^{-4}
	4	2	5.920×10^{-4}	4/1	5.920×10^{-4}
	5	2	5.830×10^{-4}	4/1	5.830×10^{-4}
	6	1	5.816×10^{-4}	3/2	5.816×10^{-4}
10^{-3}	2	6	6.121×10^{-4}	6/1	6.121×10^{-4}
	3	3	1.622×10^{-4}	6/1	1.622×10^{-4}
	4	3	7.902×10^{-5}	8/1	7.902×10^{-5}
	5	3	6.626×10^{-5}	10/1	6.626×10^{-5}
	6	2	6.432×10^{-5}	5/2	6.432×10^{-5}

ϵ	Level	NL	$\lVert u - u_{ex} \rVert$	NL/L	$\lVert u - u_{ex} \rVert$
10^{-4}	2	6	6.046×10^{-4}	6/1	6.046×10^{-4}
	3	3	1.306×10^{-4}	6/2	1.306×10^{-4}
	4	4	3.203×10^{-5}	6/5	3.206×10^{-5}
	5	3	1.110×10^{-5}	9/6	1.113×10^{-6}
	6	4	6.867×10^{-6}	7/6	6.823×10^{-6}
10^{-5}	2	6	6.045×10^{-4}	6/1	6.045×10^{-4}
	3	3	1.302×10^{-4}	6/2	1.302×10^{-4}
	4	4	3.076×10^{-5}	6/2	3.076×10^{-5}
	5	5	8.498×10^{-6}	8/12	8.498×10^{-6}
	6	15	2.443×10^{-6}	7/15	2.443×10^{-6}
0	2	6	6.045×10^{-4}	6/1	6.045×10^{-4}
	3	3	1.302×10^{-4}	6/2	1.302×10^{-4}
	4	4	3.072×10^{-5}	6/5	3.072×10^{-5}
	5	5	8.436×10^{-6}	10/15	8.436×10^{-6}
	6	17	2.274×10^{-6}	33/25	2.263×10^{-6}

Convergence rate is slower but accuracy not improved

Contents

Adaptive Step Size in Newton

$$\left[\frac{\partial \mathcal{R}(\mathcal{U}^n)}{\partial \mathcal{U}^n}\right]_j \approx \frac{\mathcal{R}(\mathcal{U}^n + \chi\delta_j) - \mathcal{R}(\mathcal{U}^n - \chi\delta_j)}{2\chi}$$

$$\delta_j = \begin{cases} 1 & \text{j-index} \\ 0 & \text{otherwise} \end{cases}$$

Choice of the free parameter χ

- **Fixed constant:** Based on the perturbation analysis on the residum[9] selected as machine precision
- **Adaptive choice:** The sensitivity study of the nonlinear behavior of power law models w.r.t. the χ, h and strength of nonlinearity[10]
  - $\chi >> \rightarrow$ loss of the advantageous quasi-quadratic convergence
  - $\chi << \rightarrow$ divergence due to numerical instabilities

Adaptive Step Size

- Effect of χ w.r.t tolerance: Number of Newton iterations for Bingham fluid flow in a channel at $\tau_s = 0.25$

χ/TOL	10^{-5}	10^{-6}	10^{-7}	10^{-8}
10^{-2}	13	16	19	22
10^{-3}	13	14	14	16
10^{-4}	14	14	15	diverge
10^{-5}	15	15	oscillate	oscillate
10^{-6}	15	oscillate	oscillate	diverge
10^{-7}	16	diverge	oscillate	diverge
10^{-8}	17	37	diverge	diverge

Adaptive Step Size

- Step size choice based on the current nonlinear reduction

$$r_n = \frac{\|\mathcal{R}(\mathcal{U}^n)\|}{\|\mathcal{R}(\mathcal{U}^{n-1})\|}$$

- Characteristic Function[11]

$$f(r_n) = 0.2 + \frac{0.4}{0.7 + \exp(1.5 r_n)}$$

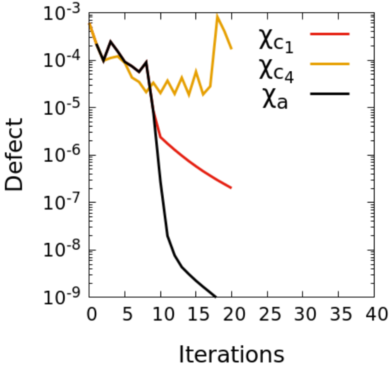

$$\boxed{Adaptive \quad \chi \longrightarrow \quad \chi_{n+1} = f^{-1}(r_n)\chi_n}$$

$\chi_c = constant \rightarrow \chi_{c_1} = 10^{-1}$, $\chi_{c_4} = 10^{-4}$ and $\chi_a = adaptive$

Contents

Bingham Flow in a Channel

Two-Field $(\boldsymbol{u}, p)$ for $\tau_s = 0.23$

$\downarrow$ **L**$/\epsilon \rightarrow$	$\mathbf{10^{-1}}$	$\mathbf{10^{-2}}$	$\mathbf{10^{-3}}$	$\mathbf{10^{-4}}$	$\mathbf{10^{-5}}$	$\mathbf{10^{-1}}$	$\mathbf{10^{-2}}$	$\mathbf{10^{-3}}$	$\mathbf{10^{-4}}$	$\mathbf{10^{-5}}$
	Newton					**Adaptive Newton**				
3	2	3	-	-	-	4	4	5	5	9
4	2	3	-	-	-	4	4	5	5	9
5	2	3	-	-	-	4	4	6	5	9

Three-Field $(\boldsymbol{u}, \boldsymbol{\sigma}, p)$ for $\tau_s = 0.23$

$\downarrow$ **L**$/\epsilon \rightarrow$	$\mathbf{10^{-1}}$	$\mathbf{10^{-2}}$	$\mathbf{10^{-3}}$	$\mathbf{10^{-4}}$	$\mathbf{10^{-5}}$	**0**	$\mathbf{10^{-1}}$	$\mathbf{10^{-2}}$	$\mathbf{10^{-3}}$	$\mathbf{10^{-4}}$	$\mathbf{10^{-5}}$	**0**
	Newton						**Adaptive Newton**					
3	2	3	4	6	9	1	2	2	2	5	1	2
4	2	3	4	8	9	1	1	2	2	4	2	2
5	1	2	3	9	5	2	1	1	1	1	3	1

Accuracy & Efficiency

Nonlinear convergence w.r.t χ for regularization-free Bingham

$\underline{\boldsymbol{\tau_s = 0.23}}$

- $h_x = \frac{1}{4}, h_y = \frac{1}{12}$
- $\chi_c = \mathit{constant}$

  $\chi_{c_1} = 10^{-1}$

  $\chi_{c_2} = 10^{-2}$

  .

  .

  .

  $\chi_{c_7} = 10^{-7}$
- $\chi_a = \mathit{adaptive}$

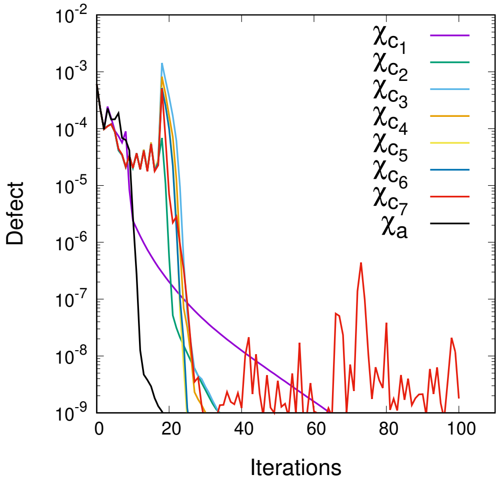

Nonlinear convergence w.r.t χ for regularization-free Bingham

$\underline{\boldsymbol{\tau_s = 0.3}}$

- $h_x = \frac{1}{4}, h_y = \frac{1}{12}$
- $\chi_c = constant$

  $\chi_{c_1} = 10^{-1}$

  $\chi_{c_2} = 10^{-2}$

  .

  .

  .

  $\chi_{c_7} = 10^{-7}$
- $\chi_a = adaptive$

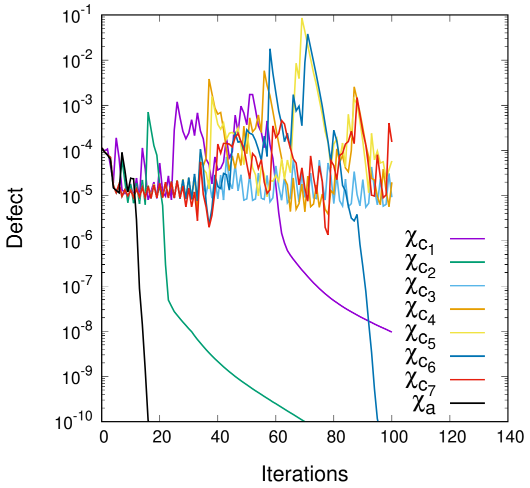

Accuracy & Efficiency

Nonlinear convergence w.r.t χ for regularization-free Bingham

$\underline{\tau_s = \mathbf{0.35}}$

- $h_x = \frac{1}{4}, h_y = \frac{1}{12}$
- $\chi_c = constant$

$\chi_{c_1} = 10^{-1}$

$\chi_{c_2} = 10^{-2}$

.

.

.

$\chi_{c_7} = 10^{-7}$

- $\chi_a = adaptive$

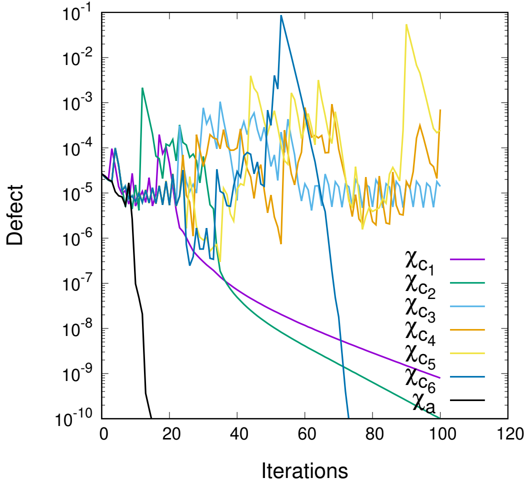

Accuracy & Efficiency

Nonlinear convergence w.r.t χ for regularization-free Bingham

$\underline{\boldsymbol{\tau_s = 0.4}}$

- $h_x = \frac{1}{4}, h_y = \frac{1}{12}$
- $\chi_c = constant$

$\chi_{c_1} = 10^{-1}$

$\chi_{c_2} = 10^{-2}$

.

.

.

$\chi_{c_7} = 10^{-7}$

- $\chi_a = adaptive$

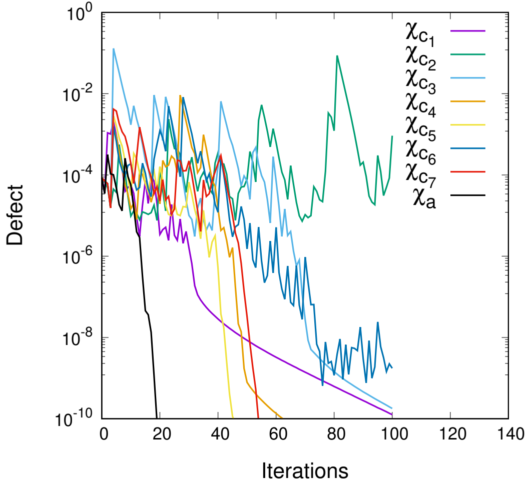

Lid Driven Cavity

- Bingham flow in a unit square $\Omega = [0, 1]^2$
- Dirichlet boundary conditions: Lid: $u_x = 1$, everywhere else $\boldsymbol{u} = 0$ at yield stress $\tau_s = 2.0$

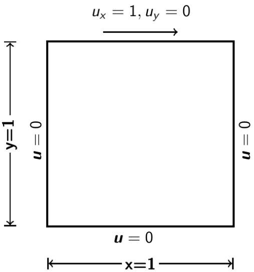

ϵ	Level	Newton	Adaptive Newton
10^{-1}	2	7	3
	3	3	3
	4	4	3
10^{-2}	2	12	4
	3	17	4
	4	11	4
10^{-3}	2	13	4
	3	21	4
	4	19	5

ϵ	Level	Newton	Adaptive Newton
10^{-4}	2	13	5
	3	21	5
	4	22	7
10^{-5}	2	13	4
	3	21	6
	4	7	7
0	2	13	5
	3	21	5
	4	18	6

Non-Yielded Zone

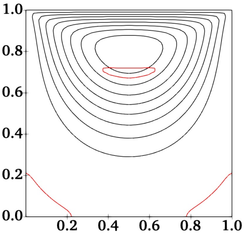

(a) $\epsilon = 10^{-1}$

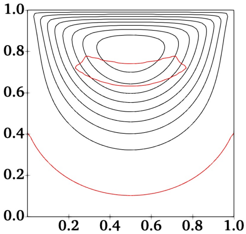

(b) $\epsilon = 10^{-2}$

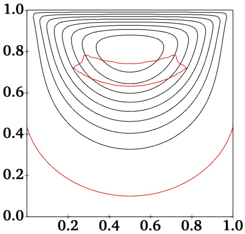

(c) $\epsilon = 10^{-3}$

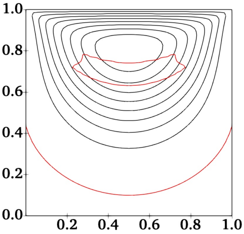

(d) $\epsilon = 10^{-4}$

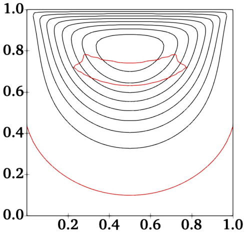

(e) $\epsilon = 10^{-5}$

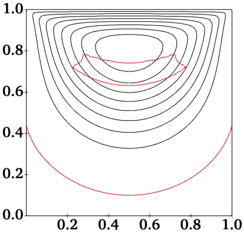

(f) $\epsilon = 0$

Validation

Figure: **Non-yielded zone:** The superposition of non yielded zone on the streamline contours for the yield stress $\tau_s = 2.0$

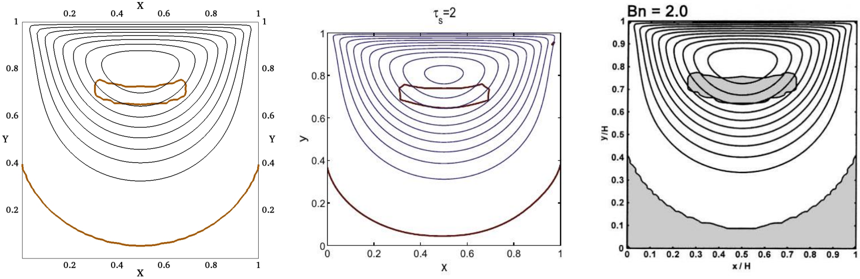

(a) Adaptive Newton (b) M. A. Olshanskii[8] (c) E. Mitsoulis[12]

Accuracy & Efficiency

Three-Field Formulation: Number of non-linear iterations for lid-driven cavity computed at the yield stress $\tau_s = 5.0$ for the Newton and adaptive discrete Newton

ϵ	Level	Newton	Adaptive Newton
10^{-1}	2	10	4
	3	11	3
	4	4	3
10^{-2}	2	21	4
	3	28	4
	4	27	3
10^{-3}	2	21	5
	3	31	5
	4	-	3

ϵ	Level	Newton	Adaptive Newton
10^{-4}	2	21	5
	3	31	6
	4	-	6
10^{-5}	2	21	5
	3	31	4
	4	-	6
0	2	5	5
	3	-	5
	4	-	6

Accuracy & Efficiency

τ_s	Level	$\epsilon = 10^{-1}$	$\epsilon = 10^{-2}$	$\epsilon = 10^{-3}$	$\epsilon = 10^{-4}$	$\epsilon = 10^{-5}$	$\epsilon = 0$
7.5	3	14	29	37	40	4	2
	4	4	5	6	6	6	6
	5	4	4	6	4	4	2
10	3	13	22	31	100	101	101
	4	4	4	4	6	12	4
	5	3	4	5	7	9	3
15	3	20	29	54	65	78	79
	4	5	5	5	5	5	5
	5	4	4	7	2	2	5

Regularization-free Bingham

$\downarrow$ L/τ_s $\rightarrow$	2	5	7.5	10	15	20	40	50
3	5	5	2	101	79	3	8	18
4	5	6	6	4	5	5	6	7
5	6	6	2	3	5	5	6	9

Non-Yielded Zone

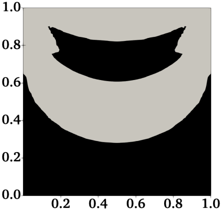

(a) $\tau_s = 10$

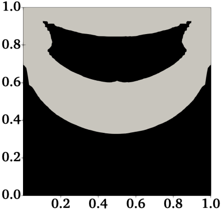

(b) $\tau_s = 15$

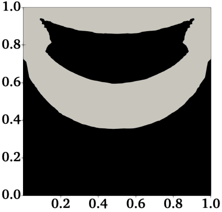

(c) $\tau_s = 20$

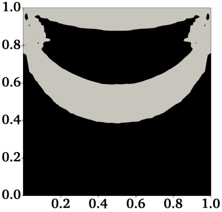

(d) $\tau_s = 30$

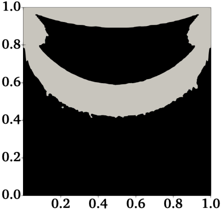

(e) $\tau_s = 40$

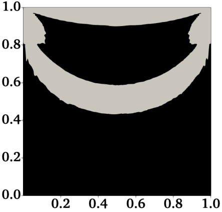

(f) $\tau_s = 50$

Rotational Bingham in a Square Reservoir

- Domain $\Omega = [0,1]^2$
- $\boldsymbol{f}(x_1, x_2) = 300\,(x_2 - 0.5, 0.5 - x_1)$
- Yield stress: $\tau_s = 14.5$
- Central solid rigid zone

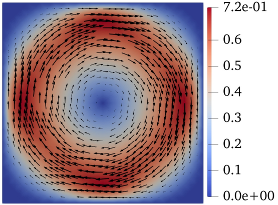

(a) Velocity field

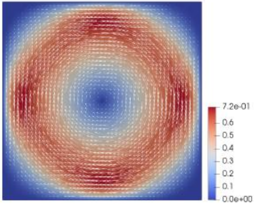

(b) Velocity field[13]

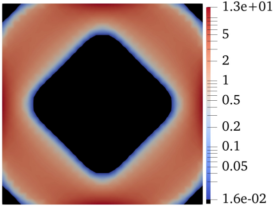

(c) Plug zones

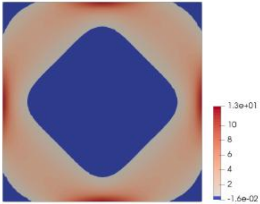

(d) Plug zones[13]

Contents

Summary

A new adaptive discrete Newton and regularization-free solver for yield stress fluids is developed

- Three-field formulation $\longrightarrow$ New auxiliary stress
- Adaptive step size $\longrightarrow$ Accurate and efficient

Advantages

- Accurate non-regularized viscoplastic solution $\longrightarrow \epsilon = 0$
- The method does not effect the shape of the yield surfaces
- Faster convergence ✓
- Significant reduction in nonlinear iterations ✓

Contents

References I

1 M. Allouche, I. A. Frigaard, and G. Sona.
Static wall layers in the displacement of two visco-plastic fluids in a plane channel.
Journal of Fluid Mechanics, 424:243–277, 2000.

2 T. C. Papanastasiou.
Flows of materials with yield.
Journal of Rheology, 31(5):385–404, 1987.

3 E.J. O'Donovan and R.I. Tanner.
Numerical study of the bingham squeeze film problem.
Journal of Non-Newtonian Fluid Mechanics, 15(1):75–83, 1984.

4 M. Bercovier and M. Engelman.
A finite-element method for incompressible non-newtonian flows.
Journal of Computational Physics, 36(3):313–326, 1980.

5 M. El-Borhamy.
Numerical Simulation for viscoplastic fluids via finite element methods.
TU Dortmund, Germany, 2012.
PhD Thesis.

6 J. Málek, V. Průša, and K.R. Rajagopal.
Generalizations of the navier–stokes fluid from a new perspective.
International Journal of Engineering Science, 48(12):1907–1924, 2010.

7 Jaroslav Hron, J. Málek, J. Stebel, and K. Touska.
A novel view on computations of steadyflows of bingham fluids using implicit constitutive relations.
August 2017.

References II

[8] A. Aposporidis, E. Haber, M. Olshanskii, and A. Veneziani.
A mixed formulation of the bingham fluid flow problem: Analysis and numerical solution.
Computer Methods in Applied Mechanics and Engineering, 200:2434–2446, 2011.

[9] C. T. Kelley.
Iterative methods for linear and nonlinear equations.
SIAM, Philadelphia, 1995.

[10] J. Hron, A. Ouazzi, and S. Turek.
A computational comparison of two FEM solvers for nonlinear incompressible flow.
In Lecture Notes in Computational Science and Engineering, volume 35, pages 87–109. Springer, 2003.
New York.

[11] S. Mandal.
Efficient FEM solver for quasi-Newtonian flow problems with application to granular material.
TU Dortmund, Germany, 2016.
PhD Thesis.

[12] Evan Mitsoulis and Thanasis Zisis.
Flow of bingham plastics in a lid-driven square cavity.
Journal of Non-newtonian Fluid Mechanics - J NON-NEWTONIAN FLUID MECH, 101:173–180, 11 2001.

[13] Sergio González, Sofía López, and Pedro Merino.
Nonsmooth exact penalization second-order methods for incompressible bingham flows.
2020.

References III

Thank you for your attention!

arooj.fatima@math.tu-dortmund.de

Regularization Models

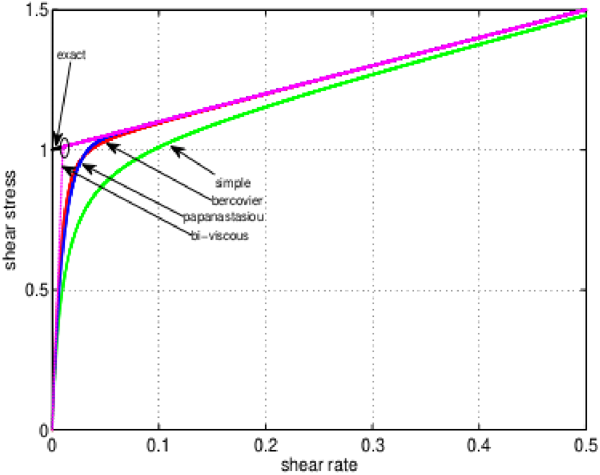

Figure: The regularization models compared with the exact Bingham model: stress versus strain rate at $\epsilon = 0.01$ and $\tau_s = 1$.